Published in final edited form as:
J Am Chem Soc. 2008 December 31; 130(52): 18008–18017. doi:10.1021/ja807331k.

Autocatalysis in Lithium Diisopropylamide-MediatedOrtholithiations

Kanwal J. Singh, **Alexander C. Hoepker**, and **David B. Collum***
Contribution from the Department of Chemistry and Chemical Biology Baker Laboratory, Cornell University, Ithaca, New York 14853-1301

Abstract

Ortholithiation of 3-fluorophenyl-*N*,*N*-diisopropyl carbamate by lithium diisopropylamide (LDA) in THF at −78 °C affords unusual rate behavior including linear decays of the carbamate, delayed formation of LDA-aryllithium mixed dimers, and evidence of autocatalysis. A mechanistic model in conjunction with numeric integration methods accounts for the time-dependent changes in concentration. The two critical rate-limiting steps in the model entail (1) an LDA dimer-based metalation of arylcarbamate, and (2) A rate-limiting condensation of the resulting aryllithium with the LDA dimer to form two isomeric LDA-ArLi mixed dimers. One isomer is elicits a highly efficient (post-rate-limiting) metalation of aryl carbamate, in turn, regenerating aryllithium. The prevalence and implications of such autocatalysis are discussed.

Introduction

Lithium diisopropylamide (LDA) is often the reagent of choice for reactions requiring a strong base.[1] The central importance of LDA motivated us to examine how solvation and aggregation influence its reactivity.[2] Studies spanning two decades have documented more than a dozen mechanisms that differ in solvation and aggregation at the rate-limiting transition structures. Recent studies of the LDA-mediated ortholithiation of aryl carbamates[3,4] underscore the potential complexity by revealing both monomer and dimer-based pathways. A pronounced autoinhibition was traced to intervening mixed aggregates, which are often observed in reactions of LDA.[5]

dbc6@cornell.edu.

Supporting Information: NMR spectra, rate and computational data, experimental protocols, details on the numeric integrations (96 pages), and a complete list of authors for ref [19]. This material is available free of charge via the Internet at http://pubs.acs.org.

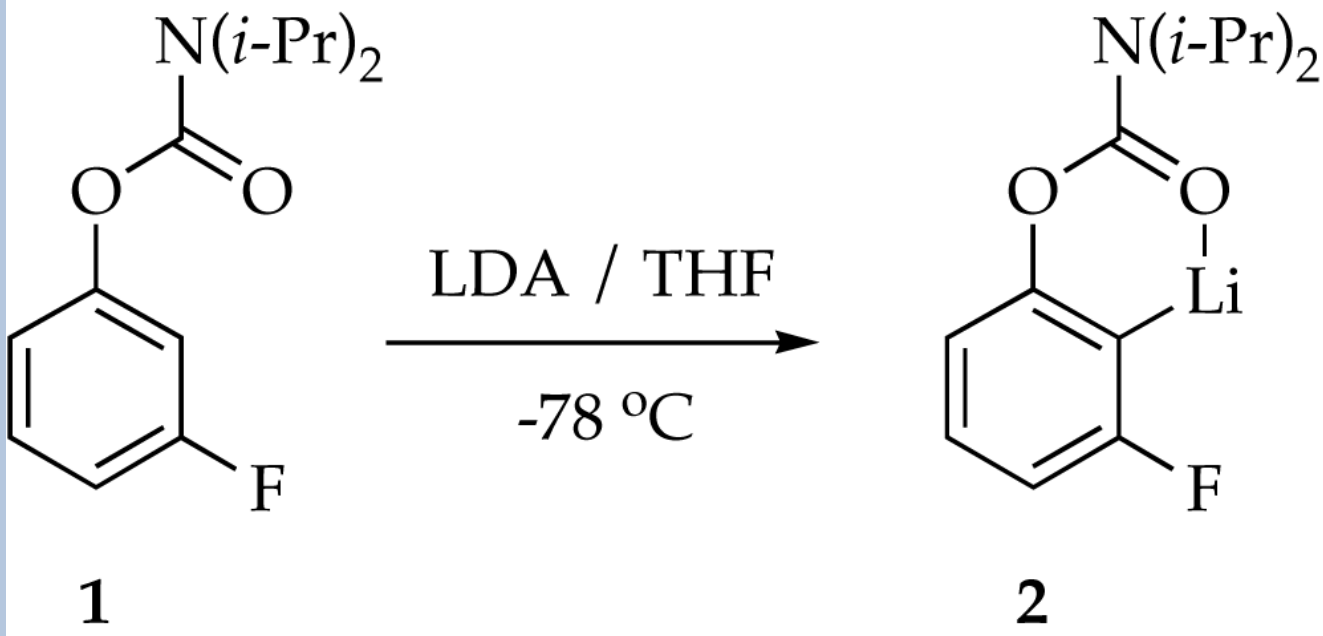

1 **2**

(1)

LDA-mediated metalation aryl carbamate **1**, the most reactive of all carbamates we had studied to date,[ref] displayed two perplexing behaviors. First, treating carbamate **1** with 1.0 equiv of LDA in neat THF at −78 °C--conditions used for many LDA-mediated reactions--affords aryllithium monomer **2** to the exclusion of mixed aggregates. The concentration of **1** also follows a first-order decay to a reasonable approximation (Figure 1); a second-order fit (dashed line) is clearly inferior. Thus, on first inspection, we appeared to have discovered the most outwardly simple LDA-mediated reaction reported to date. Something was wrong, however: This inherently bimolecular reaction should *not* be first order, regardless of whether the rate-limiting transition structure is based on an LDA monomer or dimer. The second strange observation appeared when a large excess of LDA was used. The large excess--so-called pseudo-first-order conditions--usually forces a higher-order reaction to behave as if it is first order (thus the name). When such pseudo-first-order conditions are used we observe a linear decay of **1** (Figure 2). The decay is clearly *not* first order in carbamate **1**, appearing instead to be *zeroth*-order.

We describe herein structural and rate studies showing that numerous deviant rate behaviors for the ortholithiation of **1** stem from mixed aggregates and autocatalysis[6,7] as summarized generically in Scheme 1.[5-11] It is the most mechanistically complex reaction of LDA reported to date. Autocatalysis results from intervening LDA-ArLi mixed dimers **4** and **5**. Although metalation of arene **1** by minor isomer **5** (Step III) is an important step in this unusual autocatalysis, the condensation of aryllithium **2** with LDA dimer **3** (Step IV) is rate limiting. Mounting evidence suggests that autocatalysis may be prevalent in LDA/THF-mediated reactions at −78 °C.

Results

General Methods

LDA, [^{6}Li]LDA, and [^{6}Li,^{15}N]LDA were purified as white crystalline solids.[12] The structural assignments derive from routine ^{6}Li, ^{13}C, and ^{15}N NMR spectroscopic methods.[9,13]

Rate studies were carried out using in situ IR spectroscopy[14] and ^{19}F NMR spectroscopy[15] following standard protocols. The results from the two forms of spectroscopy are fully consistent. Unless stated otherwise, pseudo-first-order conditions were established by maintaining the concentration of carbamate **1** at 0.004-0.008 M. LDA and THF were maintained at high yet adjustable concentrations using hexane as the cosolvent.[16] Although pseudo-first-order conditions are used routinely to preclude the effects of mixed aggregation and other conversion-dependent effects,[2,8b,11] mixed aggregation effects are pronounced under all conditions used to lithiate carbamate **1**.[17,18] IR spectroscopic analysis of the lithiation of carbamate **1** with >1.0 equiv of LDA in THF reveals that the reaction proceeds to full conversion. Under no conditions do we observe carbamate-LDA complexation. Time-dependent concentrations measured by ^{19}F NMR spectroscopy are fit to a mechanistic model (see Discussion) expressed by a set of differential equations (see Experimental) using numeric integration, yielding functions describing concentration versus time for multiple species.

Density functional theory (DFT) computations were carried out at the B3LYP/6-31G(d) level.[19] The isopropyl moieties of carbamate **1** were approximated with methyl groups, and THF was modeled using Me_2O. Free energies are reported in kcal/mol at −78 °C. The computational results are described sparingly in appropriate contexts below; additional results are archived in supporting information, including some calculations using LDA rather than Me_2NLi.

Solution Structures

In this section we focus only on structure; the time-dependent aggregate concentrations are examined extensively in subsequent sections. ^{6}Li and ^{15}N NMR spectroscopic studies using 2.0 equiv [^{6}Li,^{15}N]LDA reveal aryllithium **2**, LDA dimer **3**, and mixed dimer **4** (Figure 3).[13,20] An additional species (ca. 3%), putative mixed dimer **5**, was detected using ^{19}F NMR spectroscopy (below) but was not observed in the ^{6}Li spectra.

Aryllithium **2** shows no ^{15}N coupling, consistent with the absence of an LDA fragment. Limited solubility prevented ^{13}C NMR spectroscopic analysis of the ^{6}Li-^{13}C coupling, but analogous aryllithiums with ortho fluoro moieties[21] or other potentially coordinating ortho substituents are monomeric.[22] Computional studies show minima for mono- and disolvated aryllithium monomer and suggest that disolvated monomer is preferred. Mixed dimer **4** is easily assigned from ^{6}Li-^{13}C and ^{6}Li-^{15}N coupling patterns as described previously.[5a]

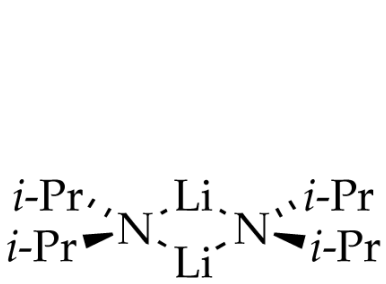

3

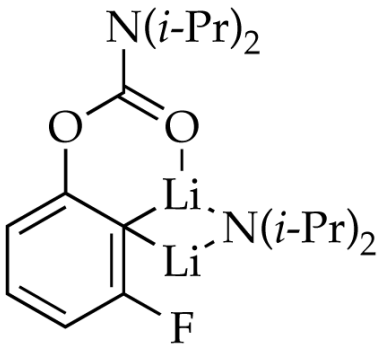

4

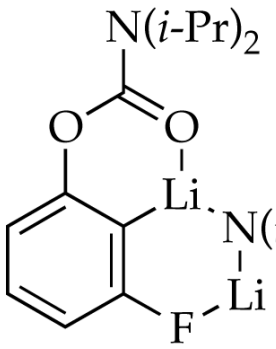

5

Monitoring ortholithiations of **1** using ^{6}Li and ^{19}F NMR spectroscopies allowed us to assign ^{19}F resonances to aryllithium monomer **2** and mixed dimer **4**; a representative spectrum is shown in Figure 4. We also observe an additional species (**5** in Figure 4) initially suspected to be a mixed trimer akin to those characterized previously.[5,8,10] The ratio of **4** and **5**, however, is invariant with large changes in ArLi, LDA, and THF concentrations (see supporting information). Thus, **4** and **5** are *isomers*.

Computations were used to investigate the solvation of **4** and the more elusive gross structure and solvation of **5** (Scheme 2). Serial solvation shows minima for mono- and disolvated mixed dimers **6**-**9**. Trisolvates failed to minimize, resulting in desolvation in each attempt. Mono- and disolvated dimers **6** and **7** are isoenergetic whereas **8** and **9** are significantly less stable. Dimer **7**, bearing a C-Li-N-Li connectivity characteristic of open dimers[23,24] but with an unusual Li-F interaction, is the only detectable structure bearing two solvents coordinated to the lithium distal to the carbamoyl moiety. No minimum was found corresponding to the analog of **7** with a single solvent on the distal lithium.

Experimental data show that **4** and **5** are isomeric, whereas computations suggest such closed and ring-expanded forms prefer different solvation numbers. We are convinced by the experimental data and, given the approximations used, are comfortable offering **9** and **7** as computational models of isomeric mixed dimers **4** and **5** (respectively). The unusual structural features in **7** reappear in calculated transition structures (vide infra) and in mechanistic discussions.

Linear Decays

In theory, the linear decay for the ortholithiation of **1** (illustrated in Figure 2) could arise if an aggregation event such as a deaggregation is rate limiting (eqs 2 and 3).[25] The rate of ortholithiation would be dictated by the rate at which monomer is formed[26] and independent of the initial substrate concentration (Figure 5).

$$(i\text{-}Pr_2NLi)_2 \underset{slow}{\overset{slow}{\rightleftharpoons}} 2i\text{-}Pr_2NLi \tag{2}$$
3

$$i\text{-}Pr_2NLi + ArH \xrightarrow{fast} [(i\text{-}Pr_2NLi)(ArH)]^{\ddagger} \tag{3}$$
1

In practice, the scenario in eqs 2 and 3 did not withstand scrutiny. Figure 6 reveals reaction rates that depend markedly on the initial concentration of the carbamate. The nearly coincident x-intercepts in Figure 6 are strikingly similar to those in plots of initial rates arising from a first-order reaction.[26] A plot of the slopes from Figure 6 versus initial substrate concentration (Figure 7) illustrates the concentration-dependent rates. The highest substrate concentrations in Figure 6 far exceed those necessary to preserve pseudo-first-order conditions, yet the linearities persist.

These results present a paradox. The linearities suggest zeroth-order substrate dependencies, but the substrate concentration-dependent slopes are akin to those for first-order substrate dependencies. Autocatalysis is the culprit.[27]

Evidence of Autocatalysis

We routinely carry out rate studies under pseudo-first-order conditions in which the substrate is kept at low concentration. By allowing no more than a 5% accumulation of new lithium salts one usually precludes autoinhibition and autocatalysis that can arise from the intervention of mixed aggregates.[2] The successful exclusion of such mixed aggregation effects is demonstrated by a simple control experiment: on completion of a reaction, injection of a second small aliquot of substrate provides a decay and a second value for k_{obsd} that is unchanged (±10%). By inference, the products of the reaction do not influence the rate or mechanism.

One might expect a second aliquot of **1** would afford an analogous linear decay that is superimposable on the first (±10%.) Experimentally, however, serial injection of two aliquots of carbamate **1** to a large excess of LDA in THF at −78 °C reveals a linear decay in the first and an almost instantaneous reaction in the second. Significant accelerations in the second aliquot are observable under many conditions studied, suggesting to us that the linear decays in Figure 6 derive, at least in part, from the superposition of autocatalysis on a normal (first-order) decay.[6] Pronounced mechanistic changes likely derive from LDA-aryllithium mixed aggregates.[28]

Autocatalysis emerged in a more conventional form[6,7] with minor changes in the reaction conditions. By example, sigmoidal curvature (anomalous acceleration) is observed at low THF concentration using hexane as a cosolvent.[29] Similar sigmoidal decays are observed for the lithiation of **1-*d*$_1$** (Figure 8). A second aliquot of **1-*d*$_1$** is consumed nearly instantaneously. Comparing the initial rates (slopes at early conversion) of **1** and **1-*d*$_1$** affords a small kinetic isotope effect (k_H/k_D = 2-3). Ortholithiations, including LDA-mediated ortholithiations of structurally related carbamates,[5] display isotope effects covering a wide range (k_H/k_D = 3 to >20).[30,31] The high reactivity of the LDA-ArLi mixed aggregates--an essential component of autocatalysis--correlates with the delayed onset on mixed aggregation as shown below.

Delayed Mixed Aggregation

Monitoring ortholithiations of **1** using ^{19}F NMR spectroscopy reveals very odd time-dependent changes in concentrations illustrated emblematically in Figures 9-11. The origins of the functions drawn through the data are described in the discussion. Several qualitative observations and control experiments are immediately noteworthy.

The linear loss of carbamate **1** in Figure 9 correlates quantitatively with appearance of aryllithium monomer **2**. Oddly, mixed dimers **4** and **5** appear after the ortholithiation of **1** is complete and quite slowly: Aggregates are not completely equilibrated on the time scale of the ortholithiation.[25] At low THF concentrations Figure 10), the mixed dimers begin to appear before the metalation of **1** is complete. The inflection point in the formation of mixed dimer **4**--the point of maximum rate--correlates with the maximum concentration of aryllithium **2**,

suggesting that **2** is a key precursor to **4**.[32] Importantly, the ratio of **4** and **5** remains constant at the equilibrium value throughout the reaction coordinate, indicating that **4** and **5** exchange rapidly on the time scale of the metalation.

Mixed dimers appeared to be the probable source of autocatalysis. Indeed, injecting carbamate **1** directly into solutions containing LDA dimer **3** and mixed dimers **4** and **5** within the NMR probe.[25] ^{19}F NMR spectroscopic analysis showed that both **4** and **5** disappear in seconds with concomitant appearance of aryllithium monomer **2** (Step III, Scheme 1). The much slower condensation of aryllithium **2** with LDA to regenerate the mixed dimers (Step IV, Scheme 1) occurs subsequently.

Temperature Effects

Ortholithiation at −100 °C (Figure 11) causes mixed dimer **4** to build to an appreciable and relatively constant concentration whereas mixed dimer **5** does not. The ratio of **4** and **5** is also *not* constant and is markedly perturbed from its equilibrium value until the carbamate is consumed. The isomerization of **4** and **5** is slow on the time scale of the metalation at −100 °C. This temperature effect proves to be important in showing that **5** is the key reactive form (vide infra).

Reaction of LDA Dimer with ArH

The first stage in teasing apart the overall mechanism is to investigate key steps individually. The method of initial rates offers insight into the reaction of LDA and carbamate **1** before the onset of autocatalysis (Step I, Scheme 1). (By virtue of the linearities illustrated in Figure 6, the slopes and initial rates are equivalent.) Using ^{19}F NMR spectroscopic data we showed a first order in LDA (Figure 12) and zeroth order in THF (Figure 13). The idealized rate law[33] in eq 4, in conjunction with the assignment of LDA dimer **3** as a disolvate,[2,9a] is consistent with the generic mechanism in eq 5. Open-dimer-based transition structure **10** is shown to be plausible by computation.[8] Analogous open-dimer-based transition structures have been implicated on many occasions.[23]

$$-d[\mathrm{ArH}]/dt = k'[\mathrm{LDA}][\mathrm{THF}]^0[\mathrm{ArH}] \tag{4}$$

$$(i\text{-}\underset{3}{\mathrm{Pr_2NLi}})_2 + \underset{1}{\mathrm{ArH}} \xrightarrow{k'} [(i\text{-}\mathrm{Pr_2NLi})_2\,\underset{10}{(\mathrm{ArH})}\,(\mathrm{THF})_2]^{\ddagger}$$

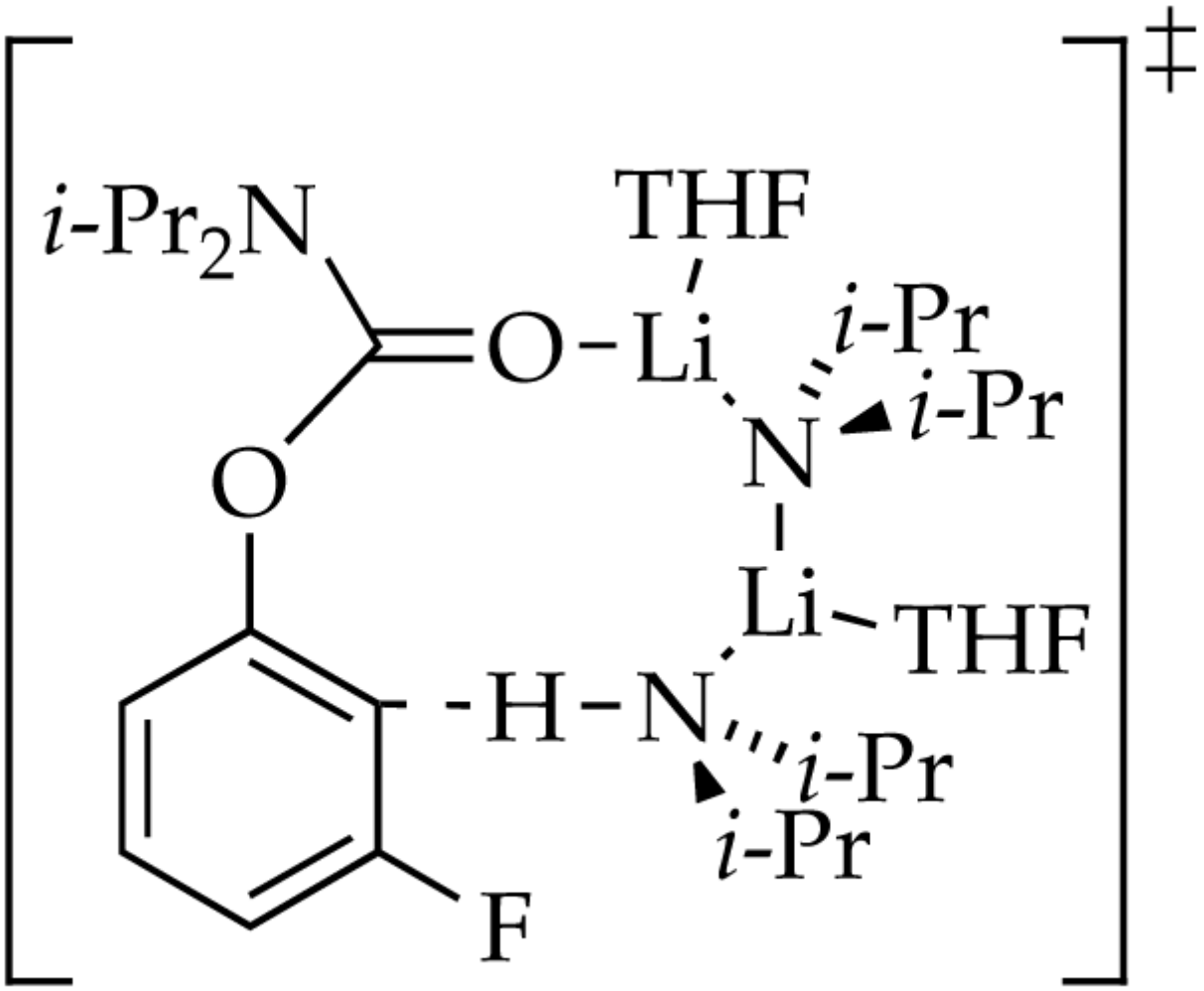

10

(5)

Reaction of LDA Dimer with ArLi

After substrate **1** is consumed, the loss of aryllithium **2** via condensation with LDA dimer **3** to form mixed dimer **4** (Step IV, Scheme 1) follows clean pseudo-first-order behavior. Analogous reactivity was observed by adding a solution of LDA dimer **3** to aryllithium monomer **2**. Monitoring the pseudo-first-order rate constants as a function of LDA and THF concentrations (Figures 14 and 15) shows that the condensation is first order in LDA and an inverse first order in THF.[34] The idealized rate law (eq 6) is consistent with a rate-limiting transition structure of stoichiometry $[(i\text{-Pr}_2\text{NLi})_2(\text{ArLi})]^{\ddagger}$ (eq 7).[35] (The THF ligands are not included because the solvation number of ArLi **2** was studied only computationally, but disolvation seems likely.) This slow aggregation event is important in the formulation of an overall mechanistic hypothesis. Although we cannot even hazard a guess as to what transition structure **11** might look like, the relationship of transition structures **10** and **11** may be important (vide infra).

$$-d[\mathrm{ArLi}]/dt = k'[\mathrm{LDA}][\mathrm{ArLi}][\mathrm{THF}]^{-1} \quad (6)$$

$$\underset{3}{(i\text{-}\mathrm{Pr_2NLi})_2} + \underset{2}{\mathrm{ArLi}} \xrightarrow{k'} [\underset{11}{(i\text{-}\mathrm{Pr_2NLi})_2(\mathrm{ArLi})}]^{\ddagger} \quad (7)$$

Reaction of Mixed Dimers with ArH

The reaction of arene **1** with the mixed dimers (Step III, Scheme 1) was too fast to obtain useful rate data as evidenced by the nearly instantaneous reaction when a carbamate **1** is added to a solution of **4** and **5**. DFT computations, however, provide insights that we find quite provocative. Given the circumstantial evidence supporting disolvation of **4** and **5**, we focused our computations on transition structures bearing the carbamate carbonyl moiety and one or two solvents. The transition structures bearing only one solvent proved to be much more stable computationally. (We have no experimental evidence to support either solvation number.) The results focusing on monosolvated transition structures **12** and **13** are illustrated in Scheme 3.

We believe the most logical scenario to explain the data at −100 °C is that **5** reacts directly with carbamate **1** (modeled by the conversion of **7** to **13**) and that **4** reacts by a rate-limiting conversion to **5** (modeled by the conversion of **9** to **7**). We not that the lack of Li-C-Li contacts in **7** and **13** is intriguing.

Discussion

We have described rate studies of the LDA-mediated metalation of carbamate **1** (eq 1). A host of observations that are unusual when placed in the context of previous mechanistic studies point to the importance of autocatalysis in which the resulting ArLi forms highly reactive mixed aggregates (Scheme 1). A summary of the key observations is followed by a detailed discussion of a mechanistic model depicted generically in Scheme 1.

Strange Rate Behavior

Ortholithiation of carbamate **1** under standard conditions--equimolar LDA in THF at −78 °C--shows a notable simplicity exemplified by an apparent first-order decay (Figure 1) and an absence of mixed aggregates. Surprisingly, metalations using >2.0 equiv of LDA display unusual linear decays of carbamate **1** to full conversion (Figure 2). Linear decays of substrate versus time typically stem from zeroth-order dependencies on substrate that occur because the substrate is *not* involved in the rate-limiting step.[7c] The carbamate concentration dependence of the decays in Figure 6, however, suggests a first-order dependence on carbamate **1**. The two conclusions seem paradoxical. Indeed, the downwardly curving (sigmoidal) decays observed when using deuterated carbamate **1** (Figure 8) or low THF concentrations suggest autocatalysis is the culprit,[29] and the high reactivities of LDA-ArLi mixed dimers are supportive.

^{19}F NMR spectroscopy offers a vivid picture of the odd time-dependent aggregate concentrations (Figures 9-11). The linear disappearance of carbamate **1** in Figure 9 correlates quantitatively with an analogous linear formation of aryllithium monomer **2**. Mixed dimer **4** and traces of isomeric mixed dimer **5** eventually appear, but only after the ortholithiation is complete. (Depiction of **5** as a fluorine-chelated open dimer[23,24] derives from computational rather than spectroscopic data.) This delayed mixed aggregation was difficult to understand at the outset.

Reducing the THF concentration Figure 10) causes aryllithium **2** to reach a lower maximum concentration and makes aggregates **4** and **5** visible before the carbamate has been fully consumed. Lowering the reaction temperature to −100 °C produces several notable changes including a measurable and surprisingly constant concentration of mixed dimer **4** but not **5** (Figure 11). The deviation of isomeric mixed dimers **4** and **5** from their equilibrium ratio is significant.

Mechanistic Model

It is an understatement to say that the conventional mechanisms for LDA-mediated reactions[2] fail to account for the results summarized above. Many unconventional models were considered and also found wanting. We offer a single model described by eqs 9-12 (referred to as simply “the model”) based on the four steps summarized in Scheme 1.

LDA Dimer-Based Metalation (Step I)

$$(i\text{-}\underset{3}{\mathrm{Pr_2NLi}})_2 + \underset{1}{\mathrm{ArH}} \xrightarrow{k_1} (i\text{-}\underset{4}{\mathrm{Pr_2NLi}})\,(\mathrm{ArLi}) + i\text{-}\mathrm{Pr_2NH} \tag{9}$$

Mixed Dimer Isomerization (Step II)

$$(i\text{-}\underset{4}{\mathrm{Pr_2NLi}})\,(\mathrm{ArLi}) \underset{k_{-2}}{\overset{k_2}{\rightleftharpoons}} (i\text{-}\underset{5}{\mathrm{Pr_2NLi}})\,(\mathrm{ArLi})^* \tag{10}$$

Mixed Dimer-Based Metalation (Step III)

$$(i\text{-}\underset{5}{\mathrm{Pr_2NLi}})\,(\mathrm{ArLi})^* + \underset{1}{\mathrm{ArH}} \xrightarrow{k_3} 2\,\underset{2}{\mathrm{ArLi}} + i\text{-}\mathrm{Pr_2NH} \tag{11}$$

LDA-ArLi Condensation (Step IV)

$$(i\text{-}\underset{3}{\mathrm{Pr_2NLi}})_2 + \underset{2}{\mathrm{ArLi}} \underset{k_{-4}}{\overset{k_4}{\rightleftharpoons}} (i\text{-}\underset{4}{\mathrm{Pr_2NLi}})\,(\mathrm{ArLi}) + 1/2(i\text{-}\underset{3}{\mathrm{Pr_2NLi}})_2 \tag{12}$$

A discussion of the model is prefaced by a few essential points. First, we used standard kinetic methods to measure the full rate laws for the key rate-limiting steps (eqs 9 and 12). The THF dependencies were also measured, but they add more complexity than clarity. Thus, we exclude them from the discussion and simply note that the model is consistent with data acquired at all THF concentrations. Similarly, the differential equations used in the numeric integrations add little to the discussion; they are presented and discussed in the experimental section.

Second, models containing large numbers of differential equations and adjustable parameters are said to be “sloppy” if they are highly under determined.[36] Can't *any* model with such a plethora of adjustable parameters fit the data? Can the model “fit an elephant and make it wag its tail”?[37] The answer is no (for the first question, at least). The model is *not* sloppy. The adjustable parameters corresponding to the six rate constants are well defined. Moreover, many other models that were poked and prodded included provisions for autocatalysis, linear (or

sigmoidal) decays, or delayed mixed aggregate formation but failed to account for *all* behaviors. The model has one compelling strength when compared with all other models that we considered and dismissed: *It fits the data in every instance*. The numeric integrations illustrated in Figures 9-11 are emblematic of the quality of the fits.

To facilitate the discussion, the model is described as four discrete steps, and the origins of each as well as the portions of the model that are negotiable are discussed. To minimize confusion we also note at the outset that, although facile mixed dimer-based lithiation of carbamate **1** is necessary, the condensation of ArLi with LDA dimer in eq 12--an aggregation event, not a metalation[25]--is the key rate-limiting step in the autocatalysis.

LDA Dimer-Based Metalation

The first stage of the metalation of carbamate **1** (Scheme 1, Step I)--the reaction before the appearance of lithium salt products--was shown using standard methods to be LDA dimer-based as described by eq 9 and represented by transition structure **10**. Temperature dependencies (discussed below) are only consistent with mixed dimer **4** as the first-formed product and isomer **5** as the key reactive form.

Mixed Dimer Isomerization

Eq 10 represents the exchange between cyclic dimer **4** and open dimer **5** (Scheme 1, Step II). Several experiments showed that at −78 °C **4** and **5** interconvert rapidly on the time scales that they are formed or consumed. By contrast, at −100 °C the rate of exchange becomes slow relative to the rate of mixed dimer-based metalations, which allows us--actually forces us--to distinguish which dimer is the reactive form (vide infra).

Mixed Dimer-Based Metalation

It almost goes without saying that an autocatalytic organolithium reaction involves highly reactive mixed aggregates as described by eq 11 (Scheme 1, Step III). Spectroscopic studies using rapid-injection methods[25a,b] confirm that the resulting mixed dimers react almost instantaneously at −78 °C. In some sense, this mixed dimer-based metalation is of lesser consequence to the model than one might suspect because it is a post-rate-limiting step. Their high reactivities, however, explain two empirical observations: (1) the delayed appearance of the mixed dimers **4** and **5**, and (2) the highly temperature sensitive concentration dependencies. Both are discussed below.

LDA-ArLi Condensation

The rate-limiting step in the autocatalysis is the condensation of aryllithium **2** with LDA dimer **3** (Scheme 1, Step IV) which proceeds via an LDA dimer-based mechanism.[35] The reaction coordinate is likely to be more complex than described by eq 12, however, in that the first-formed product is logically some form of $(i\text{-Pr}_2\text{NLi})_2(\text{ArLi})$ trimer. Whether the putative trimer is akin to previously characterized cyclic trimers is unknown, [5,9] but it is too fleeting to detect spectroscopically and is not germane to the numeric integrations.

Origins of Delayed Mixed Aggregation

Following an organolithium reaction using NMR spectroscopy reveals that the starting organolithium aggregates are replaced by new product-derived mixed and homoaggregates.[5] The aggregate distributions change as the reaction proceeds, but equilibrium populations are maintained[38] provided that aggregate exchange is rapid on the time scales of the reaction. This is not the case in the metalation of carbamate **1**. Mixed aggregates **4** and **5** appear only after carbamate **1** is consumed. The rapid metalation in eq 11 accounts for the delayed appearance

of the mixed dimers; the mixed dimers do indeed form but are consumed rapidly by carbamate **1** as they form.

Relative Mixed Dimer Reactivities

Unraveling the relative importance of isomeric mixed dimers **4** and **5** was particularly challenging. It was *very* tempting at the outset to ignore dimer **5** altogether given that **5** forms in low concentrations (≈3%). Although **5** was confirmed to be an isomer of **4**, its three-dimensional structure was assigned using exclusively DFT computations. Moreover, using data collected at −78 °C, conditions under which **4** and **5** equilibrate rapidly on the time scales of the metalation, it is not constructive to consider which is the so-called reactive form; **4** and **5** simply represent two resting states. At −100 °C, however, **4** and **5** interconvert slowly on the time scale of the metalation. Under these conditions it is valid to consider the relative reactivities of **4** and **5** toward arene **1**.

The model described in eqs 9-12 that is based on metalations by mixed dimer **5** fits the data, whereas alternative models based on the reaction of **4** do not. The alternative models fail to include provisions for the elevated and constant concentration of **4** during the consumption of carbamate at −100 °C (Figure 11). When the model presented is expanded to include provisions for reaction of both **4** *and* **5**, the fit suggests <1% contribution from a **4**-based metalation.

The most logical scenario that is fully consistent with the data is that **4** isomerizes to **5** and dimer **5** subsequently reacts with carbamate **1** (see Scheme 1). The isomerization is fast relative to the metalation at −78 °C, whereas the isomerization becomes rate limiting at −100 °C. It was in this context that we wondered whether the transition structure for the metalation may show a ring expanded motif similar to that of **5** rather than a more conventional closed form with a Li-C-Li contact as in **4**.

Computational studies of the mixed dimer-based metalation are summarized in Scheme 3. Dimers **4** and **5** are represented by simplified reactants **9** and **7**, respectively. Transition structures **12** and **13** are analogous to **9** and **7** in that conventional Li-C-Li contacts in **9** and **12** are absent in **7** and **13**. Curiously, the calculated activation energies are also qualitatively consistent with experiment. Most significant, the computations suggest that the ring expanded motif is relatively unfavorable in reactant **7** yet stabilizing in transition structure **13**.

Origins of Linear Decays

The model reproduces the linear decays by superimposing a downward curvature from autocatalysis on the normal upward curvature resulting from loss of substrate.[27] That is not to say, however, that it is obvious *why* the model is successful or why the linearities persist over a wide range of initial LDA concentrations. This coincidence requires elaboration as follows.

Using some abstraction we can distill the model to its simplest components. In the absence of autocatalysis, the metalation proceeds via an LDA dimer-based mechanism (eq 9). Let us recast this as eq 13 and the affiliated rate constant as k_{init}. Similarly, the autocatalytic pathway occurs via an LDA dimer-based rate-limiting condensation with ArLi. The autocatalysis simplifies to eq 14 with a rate constant denoted as k_{cat}.

$$(i-\mathrm{Pr_2NLi})_2+\mathrm{ArH}\xrightarrow{\longrightarrow}\mathrm{product} \tag{13}$$

$$(i\text{-}Pr_2NLi)_2 + ArLi \xrightarrow{\rightarrow} product \quad (14)$$

If only the uncatalyzed ortholithiation in eq 13 is operative, the reaction will follow a normal exponential decay (Figure 16, curve A). At 50% conversion of ArH, the reaction rate (the tangent to the curve A) would be 50% of the initial rate. For autocatalysis to straighten curve A to perfect linearity (curve B), the deceleration caused by the depletion of ArH must be precisely offset by the acceleration caused by the buildup of ArLi (eq 14). *Linearity is observed when* $k_{init}=k_{cat}$. Indeed, inspection of Figure 9 shows that the instantaneous slopes for the loss of carbamate **1** at early conversion and the loss of aryllithium monomer **2** (the initial slope to the right of its apex) are equal.

Is it a coincidence that the rates of the uncatalyzed and the catalyzed ortholithiation are equal? On one level, yes. Decreasing the THF concentration or introducing orthodeuteration results in sigmoidal behavior consistent with a relatively higher rate for the catalyzed process (Figure 16, curve C). (k_{init} is isotopically sensitive whereas k_{cat} is not.) Nonetheless, through the reductionist approach described by eqs 13 and 14, one can see haunting similarities. Is there a common reactive intermediate such as an LDA open dimer[23] that reacts with ArH or ArLi (eq 15) with nearly equal efficacy? Although it is unclear why the ArH and ArLi react so similarly (and certainly further speculation is getting excessive), we wonder whether the Lewis basic[39] fluoro moieties are important.

$$(i\text{-}Pr_2NLi)_2 \rightleftharpoons (i\text{-}Pr_2NLi)_2{}^* \xrightarrow{ArH \text{ or } ArLi} products \quad (15)$$

Conclusion

LDA continues to harbor mysteries and offer insights into how aggregation and solvation influence organolithium reactivity. The LDA-mediated ortholithiation delineated in eq 1 revealed linear and sigmoidal decays--evidence of autocatalysis--and exceptional reactivities of mixed aggregates that are unexpected in the context of previously studied LDA-mediated metalations.[2] The model presented, although somewhat flexible in detail and vulnerable to revision, nicely accounts for the odd observations.

Taking a wider view, these results are not merely curiosities. As we peer into the past, we are reminded of LDA-mediated enolizations in THF at −78 °C[10c,40,41] in which LDA-lithium enolate mixed aggregates markedly altered *E*/*Z* selectivities.[42] We can also offer a peek into the future. Ongoing studies are uncovering many ortholithiations that are autocatalytic. Both the similarities and substrate-dependent differences are striking. We have also discovered that Michael additions to unsaturated esters, imine metalations, and ester enolizations display such anomalous behavior.[43] All of these reactions share a common denominator: They are effected using LDA in THF at −78 °C. This is exciting from a mechanistic perspective. The prevalence of the autocatalysis, however, is also disquieting given the importance of this particular base-solvent-temperature combination in organic chemistry.

Experimental Section

Reagents and Solvents

THF, hexane, and pentane were distilled from blue or purple solutions containing sodium benzophenone ketyl. The hydrocarbon stills contained 1% tetraglyme to dissolve the ketyl. LDA was prepared from *n*-BuLi and subsequently rescrystallized.[12] The purified LDA was

shown by both potentiometry[44] and ion chromatography[45] to contain ≤0.02% LiCl. Air- and moisture-sensitive materials were manipulated under argon or nitrogen using standard glove box, vacuum line, and syringe techniques. Solutions of *n*-BuLi and LDA were titrated for active base using a literature method.[46]

NMR Spectroscopic Analyses

All NMR tubes were prepared using stock solutions and sealed under partial vacuum. Standard ^{6}Li, ^{13}C, ^{15}N, and ^{19}F NMR spectra were recorded on a 500 MHz spectrometer at 73.57, 125.79, 50.66 and 470.35 MHz (respectively). The ^{6}Li, ^{13}C, ^{15}N, and ^{19}F resonances are referenced to 0.30 M [^{6}Li]LiCl/MeOH at −90 °C (0.0 ppm), the *C*H_2O resonance of THF at −90 °C (67.57 ppm), neat Me_2NEt at −90 °C (25.7 ppm), and C_6H_5F in neat THF at −78 °C (−113.15 ppm), respectively.

IR Spectroscopic Analyses

Spectra were recorded using an in situ IR spectrometer fitted with a 30-bounce, silicon-tipped probe. The spectra were acquired in 16 scans at a gain of 1 and a resolution of 8 cm^{-1}. A representative reaction was carried out as follows: The IR probe was inserted through a nylon adapter and FETFE O-ring seal into an oven-dried, cylindrical flask fitted with a magnetic stir bar and a T-joint. The T-joint was capped by a septum for injections. Following evacuation under full vacuum and flushing with N_2, the flask was charged with a solution of LDA (108.2 mg, 1.01 mmol) in THF (10.0 mL) and cooled in a freshly prepared dry ice/acetone cooling bath. (Condensation of moisture adversely affects temperature consistency.) After recording a background spectrum, carbamate **1** was added to the LDA/THF mixture at −78 °C from a dilute stock solution (100 μL, 0.404 M) with stirring. IR spectra were recorded over the course of the reaction. To account for mixing and temperature equilibration, spectra recorded in the first 1.5 min were discarded. All reactions were monitored to >5 half-lives.

Rate Studies Using ^{19}F NMR Spectroscopy

The rates of metalation and mixed aggregation were monitored using ^{19}F NMR spectroscopy. Spectroscopic samples were prepared using either standard methods described previously or by injecting carbamate **1** via 25 μm ID flexible capillary tubing directly into the solution of LDA at −78 °C in the NMR probe.[25a,b] The methyl ^{1}H resonances on the magnetically inequivalent *i*-propyl groups on carbamate **1** coalesce on warming above −70 °C as described previously. Monitoring the decoalescence to give two distinct resonances showed that the temperature equilibration occurs in <30 s. T1 relaxation times were determined for all species, and the delay between scans was set to > 5 × T1 to ensure accurate integrations.

The condensation of **2** with LDA to form mixed aggregates **4** and **5** was easily monitored in situ because the condensation occurs only after **1** is consumed. Loss of **2** followed clean exponential decays, and formation of **4** correlated quantitatively. Results obtained from fitting the decay of **2** [$A = A_0\exp(-k_{obsd}t) + C$] or formation of **4**{$A = A_0[1 - \exp(-k_{obsd}t)]$} afforded equivalent first-order rate constants (±10 %).

Numeric Integrations

The proposed mechanism (eqs 9-13) can be expressed as a series of differential equations as follows:

$$d[\mathrm{ArH}]/dt = -k_1[\mathrm{ArH}][\mathrm{A}_2] - k_3[\mathrm{A}\cdot\mathrm{ArLi}^*][\mathrm{ArH}] \quad (16)$$

$$d[\mathrm{ArLi}]/dt = -k_4[\mathrm{ArLi}][\mathrm{A_2}] + k_{-4}[\mathrm{A\cdot ArLi}][\mathrm{A_2}]^{0.5} + 2k_3[\mathrm{A\cdot ArLi^*}][\mathrm{ArH}] \quad (17)$$

$$d[\mathrm{A\cdot ArLi}]/dt = k_1[\mathrm{ArH}][\mathrm{A_2}] - k_2[\mathrm{A\cdot ArLi}] + k_{-2}[\mathrm{A\cdot ArLi^*}] + k_4[\mathrm{ArLi}][\mathrm{A_2}] - k_{-4}[\mathrm{A\cdot ArLi}][\mathrm{A_2}]^{0.5} \quad (18)$$

$$d[\mathrm{A\cdot ArLi^*}]/dt = k_2[\mathrm{A\cdot ArLi}] - k_{-2}[\mathrm{A\cdot ArLi^*}] - k_3[\mathrm{A\cdot ArLi^*}][\mathrm{ArH}] \quad (19)$$

$$[\mathrm{A_2}] = [\mathrm{A_2(init)}] - 0.5[\mathrm{ArLi}] - [\mathrm{A\cdot ArLi}] - [\mathrm{A\cdot ArLi^*}] \quad (20)$$

where A_2 is LDA dimer **3**, ArH is arene **1**, ArLi is monomer **2**, A·ArLi is mixed dimer **4**, A·ArLi* is mixed dimer **5**, and $[A_2(init)]$ is the initial concentration of LDA.

The time-dependent concentration plots obtained by ^{19}F NMR spectroscopy are fit to a mechanistic model expressed by a set of differential equations. The curve fitting operation minimizes chi-square in searching for the coefficient values (rate constants). The Levenberg-Marquardt algorithm[47] is used for the chi-square minimization and is a form of nonlinear, least-squares fitting. The fitting procedure implements numeric integration based on the backward differentiation formula (BDF)[48] to solve the differential equations, yielding functions describing concentration versus time.

The results from the fits are as follows. From a single run, the rate constant for the LDA dimer-based metalation (k_1 in eq 9) can be uniquely determined. The equilibrium constant for the exchange of mixed dimers **4** and **5** (k_2/k_{-2}) is also well defined, yet only a lower limit can be established for the individual values of k_2 and k_{-2} (k_2, $k_{-2} > 10 \cdot k_1$). The rate constant corresponding to metalation of carbamate **1** by mixed dimer **5** (k_3 in eq 11) has a lower boundary ($>10^5 \cdot k_1$). The k_4/k_{-4} ratio corresponding to the monomer-mixed dimer equilibrium (eq 12) is well defined as are the separate values of k_4 and k_{-4}. By carrying out a global fit of multiple data sets, the quality of the individual fits are decreased somewhat as expected for a reaction that is sensitive to initial conditions. We find, however, that best-fit values of the rate constants from the global fit do not differ much from the individual fits.

The data recorded at −100 °C offer insights into the relative rate constants unavailable at −78 °C (vide infra). The individual values of k_2 and k_{-2} become well defined, which ultimately leads to the conclusion that LDA dimer-mediated metalation affords **4** and the mixed dimer-mediated metalation proceeds via **5** as described in the discussion.

Supplementary Material

Refer to Web version on PubMed Central for supplementary material.

Acknowledgments

We thank the National Institutes of Health (GM 39764) for direct support of this work and Merck, Pfizer, Boehringer-Ingelheim, R. W. Johnson, Sanofi-Aventis, Schering-Plough, and Dupont Pharmaceuticals (Bristol-Myers Squibb) for indirect support. We also thank Emil Lobkovsky for help with the crystal structure determinations and Professor Melissa Hines for help with curve fitting.

References and Footnotes

1. Bakker, WII.; Wong, PL.; Snieckus, V. Lithium Diisopropylamide. In: Paquette, LA., editor. e-EROS. John Wiley; New York: 2001. Clayden, J. Organolithiums: Selectivity for Synthesis. Baldwin, JE.; Williams, RM., editors. Pergamon; New York: 2002.
2. For a review summarizing rate studies of LDA-mediated reactions: Collum DB, McNeil AJ, Ramirez A. Angew. Chem., Int. Ed 2007;46:3002.
3. Hartung, CG.; Snieckus, V. Modern Arene Chemistry. Astruc, D., editor. Wiley-VCH; Weinheim: 2002. Chapter 10. (b) MacNeil SL, Wilson BJ, Snieckus V. Org. Lett 2006;8:1133. [PubMed: 16524286]
4. Reviews of ortholithiation: (a) Snieckus V. Chem. Rev 1990;90:879. (b) Gschwend HW, Rodriguez HR. Organic React 1979;26:1.Also, see ref [8]
5. (a) Sun X, Collum DB. J. Am. Chem. Soc 2000;122:2459. (b) Ramirez A, Sun X, Collum DB. J. Am. Chem. Soc 2006;128:10326. [PubMed: 16881665]
6. Nudelman NS, Velurtas S, Grela MA. J. Phys. Org. Chem 2003;16:669.Alberts AH, Wynberg H. J. Am. Chem. Soc 1989;111:7265.Alberts AH, Wynberg H. J. Chem. Soc., Chem. Commun 1990:453.Xie L, Saunders WH. J. Am. Chem. Soc 1991;113:3123.
7. (a) Besson C, Finney EE, Finke RG. J. Am. Chem. Soc 2005;127:8179. [PubMed: 15926847] (b) Besson C, Finney EE, Finke RG. Chem. Mater 2005;17:4925. (c) Huang KT, Keszler A, Patel N, Patel RP, Gladwin MT, Kim-Shapiro DB, Hogg N. J. Biol. Chem 2005;280:31126. [PubMed: 15837788] (d) Huang Z, Shiva S, Kim-Shapiro DB, Patel RP, Ringwood LA, Irby CE, Huang KT, Ho C, Hogg N, Schechter AN, Gladwin MT. J. Clin. Invest 2005;115:2099. [PubMed: 16041407] (e) Tanj S, Ohno A, Sato I, Soai K. Org. Lett 2001;3:287. [PubMed: 11430056] (f) Barrios-Kabderism F, Carrow BP, Hartwig. J. Am. Chem. Soc 2008;130:5842. [PubMed: 18402444]
8. (a) Singh KJ, Collum DB. J. Am. Chem. Soc 2006;128:13753. [PubMed: 17044703] (b) Ma Y, Collum DB. J. Am. Chem. Soc 2007;129:14818. [PubMed: 17985891]
9. (a) Collum DB. Acc. Chem. Res 1993;26:227. (b) Pratt LM. Mini-Rev. Org. Chem 2004;1:209.
10. (a) Romesberg FE, Collum DB. J. Am. Chem. Soc 1994;116:9198. (b) Hall PL, Gilchrist JH, Harrison AT, Fuller DJ, Collum DB. J. Am. Chem. Soc 1991;113:9575. (c) Galiano-Roth AS, Kim Y-J, Gilchrist JH, Harrison AT, Fuller DJ, Collum DB. J. Am. Chem. Soc 1991;113:5053. (d) Sun C, Williard PG. J. Am. Chem. Soc 2000;122:7829.
11. (a) Depue JS, Collum DB. J. Am. Chem. Soc 1988;110:5524. (b) McNeil AJ, Toombes GES, Gruner SM, Lobkovsky E, Collum DB, Chandramouli SV, Vanasse BJ, Ayers TA. J. Am. Chem. Soc 2004;126:16559. [PubMed: 15600361]
12. Kim Y-J, Bernstein MP, Galiano-Roth AS, Romesberg FE, Fuller DJ, Harrison AT, Collum DB, Williard PG. J. Org. Chem 1991;56:4435.
13. Spectral data: ^{6}Li NMR; **2** (ζ1.27, s), **3** (ζ1.97, t, J = 5.0 Hz), **4** (ζ1.79, d, J = 5.3 Hz). ^{13}C NMR; **4** (ζ150.5, dq, J = 121.7, 5.6 Hz). ^{15}N NMR; **3** (ζ74.7, q, J = 5.0), **4** (ζ76.4, q, J = 5.3). ^{19}F NMR; **1** (ζ −113.0, −113.2), **2** (ζ−74.5), **4** (ζ−79.4), **5** (ζ−80.5). ^{6}Li and ^{15}N NMR spectra were recorded in 11.1 M THF/pentane at −90 °C, ^{13}C NMR spectra were recorded in 3.1 M THF/pentane at −90 °C, ^{19}F NMR spectra were recorded in 11.1 M THF/pentane at −78 °C. All ^{19}F NMR resonances correspond to singlets.
14. Rein AJ, Donahue SM, Pavlosky MA. Curr. Opin. Drug Discov. Develop 2000;3:734.
15. ^{19}F NMR spectroscopy proved particularly useful in following the 1,2-additions to fluorinated quinazolinones. (a) Briggs TF, Winemiller MD, Collum DB, Parsons RL Jr. Davulcu AK, Harris GD, Fortunak JD, Confalone PN. J. Am. Chem. Soc 2004;126:5427. [PubMed: 15113214] (b) Gakh YG, Gakh AA, Gronenborn AM. Magn. Reson. Chem 2000;38:551.For a review of structural studies using ^{19}F NMR spectroscopy, see
16. The concentration of LDA, although expressed in units of molarity, refers to the concentration of the monomer unit (normality).
17. Carbamate **1** and structurally related diisopropylamine-derived carbamates and carboxamides[18] display distinct conformational properties that are not observed in less sterically congested analogues. Carbamate **1** affords normal NMR spectra at ambient temperature. On cooling the NMR probe below −70 °C, the single ^{19}F resonance (−113.1 ppm) appears as a pair of resonances (−113.2 and −113.0

ppm) in equal proportions. Similarly in the ^{13}C NMR spectrum, two methyne resonances of the diisopropyl moiety are observed at ambient temperatures whereas four are observed at ≤ −90 °C. One can explain these results by assuming a slow conformer exchange illustrated below and discussed previously.[18] A crystal structure of **1** affords the following structure displaying a highly typical orientation of the diisopropyl moiety.

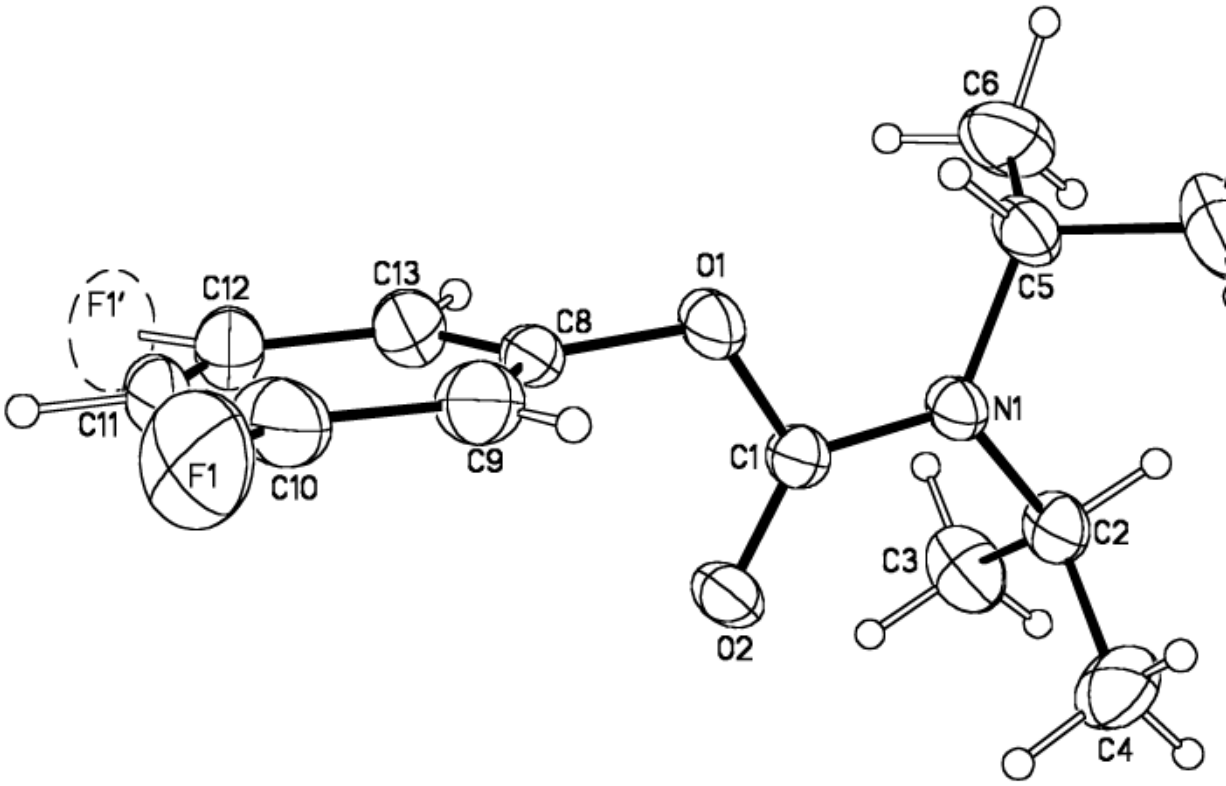

We have no evidence that conformation influences the mathematical form of the rate law described herein. To the contrary, the conformers are shown to maintain the equilibrium proportions throughout the course of the reaction.

18. For leading references to conformational studies of acylated diisopropylamido fragments, see: (a) Stewart WE, Siddall TH III. Chem. Rev 1970;70:517. (b) Lidén A, Roussel C, Liljefors T, Chanon M, Carter RE, Metzger J, Sandström J. J. Am. Chem. Soc 1976;98:2853.

19. Frisch, MJ., et al. Gaussian 03; revision B.04. Gaussian, Inc.; Wallingford, CT: 2004.

20. The structurally analogous form derived from the *N*,*N*-dimethyl carbamate derivative[8] shows two resonances (1:1) at −130 °C, consistent with the presence of the chelate.

21. Ramirez A, Candler J, Bashore CG, Wirtz MC, Coe JW, Collum DB. J. Am. Chem. Soc 2004;126:14700. [PubMed: 15535677]

22. (a) Stratakis M, Wang PG, Streitwieser A. J. Org. Chem 1996;61:3145. [PubMed: 11667177] (b) Reich HJ, Green DP, Medina MA, Goldenberg WS, Gudmundsson BÖ, Dykstra RR, Phillips NH. J. Am. Chem. Soc 1998;120:7201.

23. Open dimers were first proposed for the isomerization of oxiranes to allylic alcohols by mixed metal bases: Mordini A, Rayana EB, Margot C, Schlosser M. Tetrahedron 1990;46:2401. For a bibliography of lithium amide open dimers, see ref [5b].
24. We have also detected an analogous open dimer-based transition structure bearing a chelated meta substituent for the Snieckus-Fries rearrangement of mixed dimer **9**.
25. For examples of reactions that are fast relative to the rates of aggregate-aggregate exchanges see: (a) McGarrity JF, Ogle CA. J. Am. Chem. Soc 1985;107:1810. (b) Jones AC, Sanders AW, Bevan MJ, Reich HJ. J. Am. Chem. Soc 2007;129:3492. [PubMed: 17341084] (c) Thompson A, Corley EG, Huntington MF, Grabowski EJJ, Remenar JF, Collum DB. J. Am. Chem. Soc 1998;120:2028.
26. Espenson, JH. Chemical Kinetics and Reaction Mechanisms. Vol. 2nd ed.. McGraw-Hill; New York: 1995. p. 44Chapter 2Atkins, PW.; Jones, LL. Chemical Principles: the Quest for Insight. Vol. 2nd ed.. W H. Freeman; New York: 2002.
27. For other examples of odd linearities that may or may not have origins similar to those described herein, see: (a) Blackmond DG, Ropic M, Stefinovic M. Org. Proc. Res. Develop 2006;10:457. (b) Akao A, Nonoyama N, Mase T, Yasuda N. Org. Proc. Res. Develop 2006;10:1178. (c) Rowley JM, Lobkovsky EB, Coates GW. J. Am. Chem. Soc 2007;129:4948. [PubMed: 17397149] (d) Yin C-X, Finke RG. J. Am. Chem. Soc 2005;127:13988. [PubMed: 16201821]
28. Addition of excess *i*-Pr_2NH to the metalation has no measurable effect on the rates or curvatures.
29. Sigmoidal curvature for the loss of aryl carbamate is also observed using tetrahydropyran and 2-methyltetrahydrofuran.
30. (a) Chadwick ST, Rennels RA, Rutherford JL, Collum DB. J. Am. Chem. Soc 2000;122:8640. (b) Anderson DR, Faibish NC, Beak P. J. Am. Chem. Soc 1999;121:7553.
31. (a) Dyke AM, Gill DM, Harvey JN, Hester AJ, Lloyd-Jones GC, Munoz MP, Shepperson IR. Angew. Chem., Int. Ed 2008;47:5067. (b)Metalation of carbamate **1** in *t*-BuOMe proceeds from an LDA-carbamate complex via a normal (first-order) disappearance and displays k_H/k_D = 3-4
32. Hughes E. J. Chem. Educ 1989;66:46.
33. We define the idealized rate law as that obtained by rounding the observed reaction orders to the nearest rational order.
34. The rates rose with decreasing THF concentrations, although the high rates precluded a quantitative study. A seemingly analogous inverse THF dependence for the reaction of an aryllithium has been reported.[21]
35. The rate law provides the stoichiometry of the transition structure relative to that of the reactants: Edwards JO, Greene EF, Ross J. J. Chem. Educ 1968;45:381.
36. Brown KS, Sethna JP. Phys. Rev. E 2003;68:021904.
37. A discussion and attribution of this famous aphorism is found in reference [36]. Physicists, apparently with considerable free time, are reputed to have successfully drawn elephants using complex mathematics and numerous adjustable parameters.
38. (a) Casado J, Lopez-Quintela MA, Lorenzo-Barral FM. J. Chem. Educ 1986;63:450. (b) Alberty RA. J. Chem. Educ 2004;81:1206.Hammes, GG. Principles of Chemical Kinetics. Academic Press; New York: 1978. p. 14-15.
39. Through-space Li-F interactions have been detected. (a) Stalke D, Klingebiel U, Sheldrick GM. Chem. Ber 1988;121:1457. (b) Armstrong DR, Khandelwal AH, Kerr LC, Peasey S, Raithby PR, Shields GP, Snaith R, Wright DS. Chem. Commun 1998:1011. (c) Plenio H, Diodone R. J. Am. Chem. Soc 1996;118:356. (d) Henderson KW, Dorigo AE, Liu Q-Y, Williard PG. J. Am. Chem. Soc 1997;119:11855. (e) Kessar SV, Singh P, Singh KN, Bharatam PV, Sharma AK, Lata S, Kaur A. Angew. Chem., Int. Ed 2008;47:4703.
40. For leading references and discussions of mixed aggregation effects, see: (a) Seebach D. Angew. Chem., Int. Ed. Engl 1988;27:1624. (b)TchoubarBLoupyASalt Effects in Organic and Organometallic Chemistry1992VCHNew YorkChapters 4, 5, and 7 (c) Briggs TF, Winemiller MD, Xiang B, Collum DB. J. Org. Chem 2001;66:6291. [PubMed: 11559177] (d) Caubère P. Chem. Rev 1993;93:2317.
41. Hall PL, Gilchrist JH, Collum DB. J. Am. Chem. Soc 1991;113:9571.
42. Xie and Saunders also observed oddly variable isotope effects on the enolization. Xie L, Saunders WH Jr. J. Am. Chem. Soc 1991;113:3123.

43. Collum DB, Singh K, Viciu M, Ramirez A, Yun M. unpublished (b) Liao S, Collum DB. J. Am. Chem. Soc 2003;125:15114. [PubMed: 14653747]Hints of linear decays were noted in metalations of imines by LDA/THF at −78 °C

44. Evans, A. Potentiometry and Ion-Selective Electrodes. Wiley; New York: 1987.

45. Fuji T. Anal. Chem 1992;64:775.

46. Kofron WG, Baclawski LM. J. Org. Chem 1976;41:1879.

47. For an explanation of the Levenberg-Marquardt nonlinear least-squares optimization, see: PressWHFlanneryBPTeukolskySAVetterlingVTNumerical Recipes in C1988Cambridge University PressLondonChapter 14.4

48. Brown PN, Byrne GD, Hindmarsh AC. J. Sci. Stat. Comput 1989;10:1038.

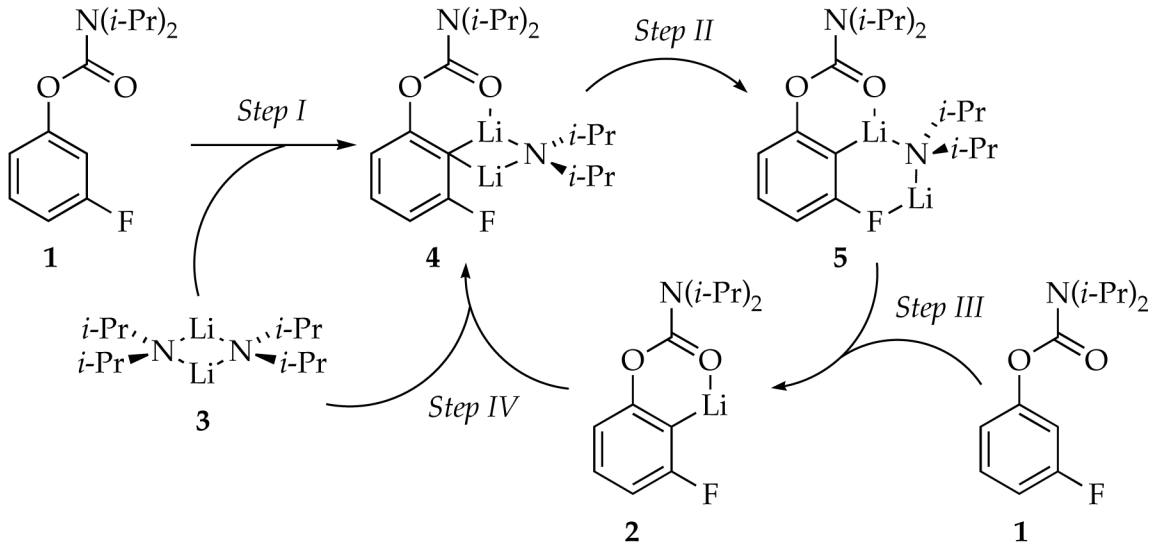

Scheme 1.

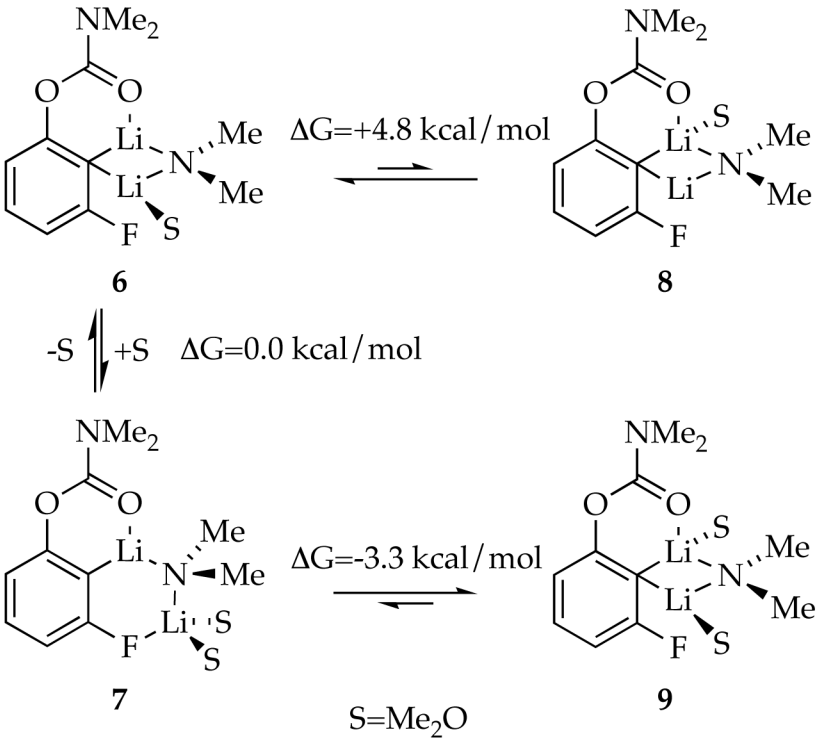

Scheme 2.

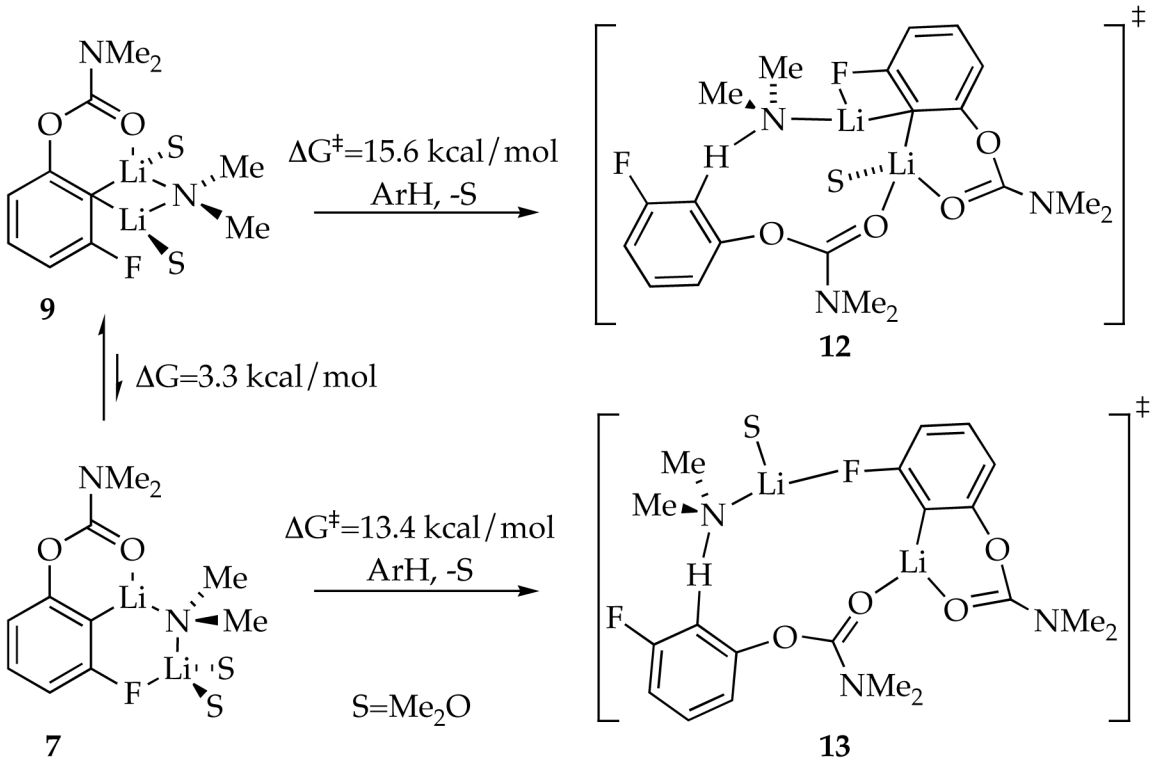

Scheme 3.

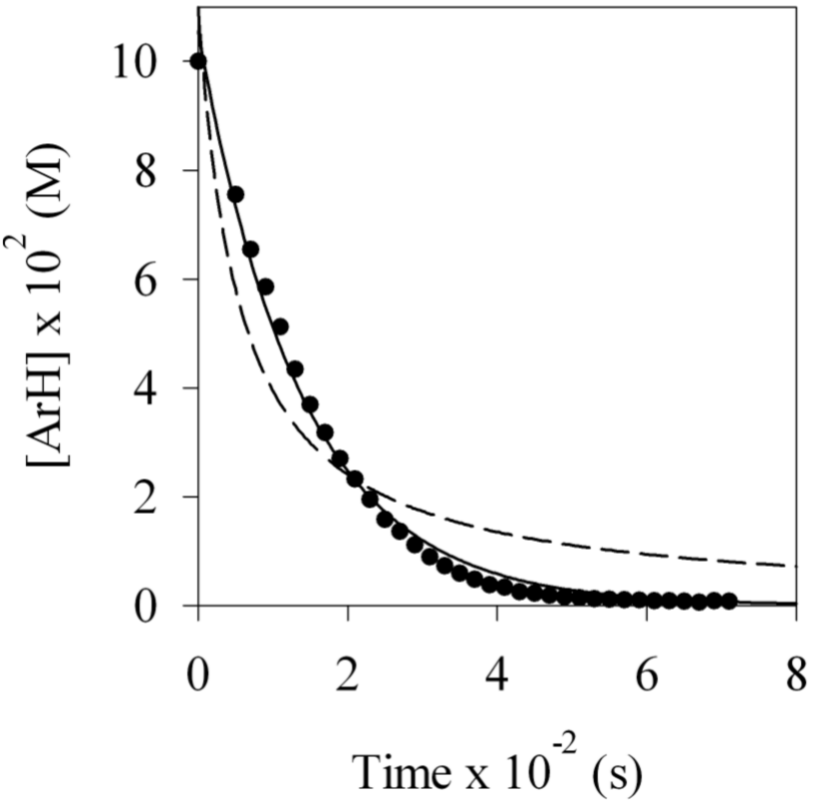

Figure 1.
Reaction of 0.10 M carbamate **1** with 0.10 M LDA at −78 °C in neat THF as monitored by ^{19}F NMR spectroscopy. The solid and dashed lines represent least squares fits to first and second order decays, respectively.

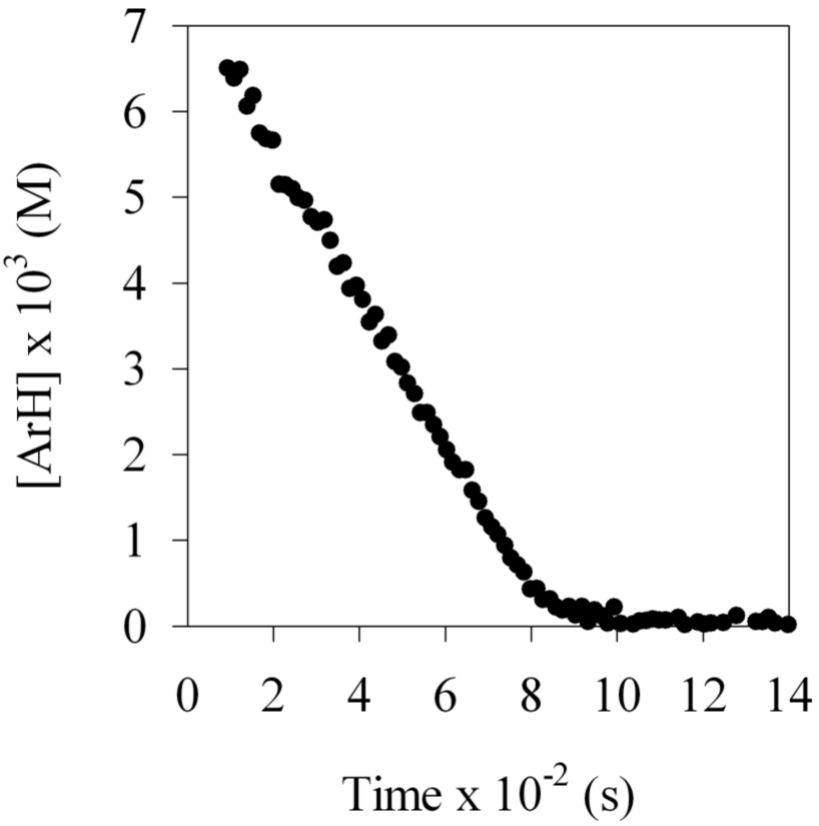

Figure 2.
Reaction of 0.010 M carbamate **1** with 0.10 M LDA at −78 °C in neat THF as monitored by ^{19}F NMR spectroscopy.

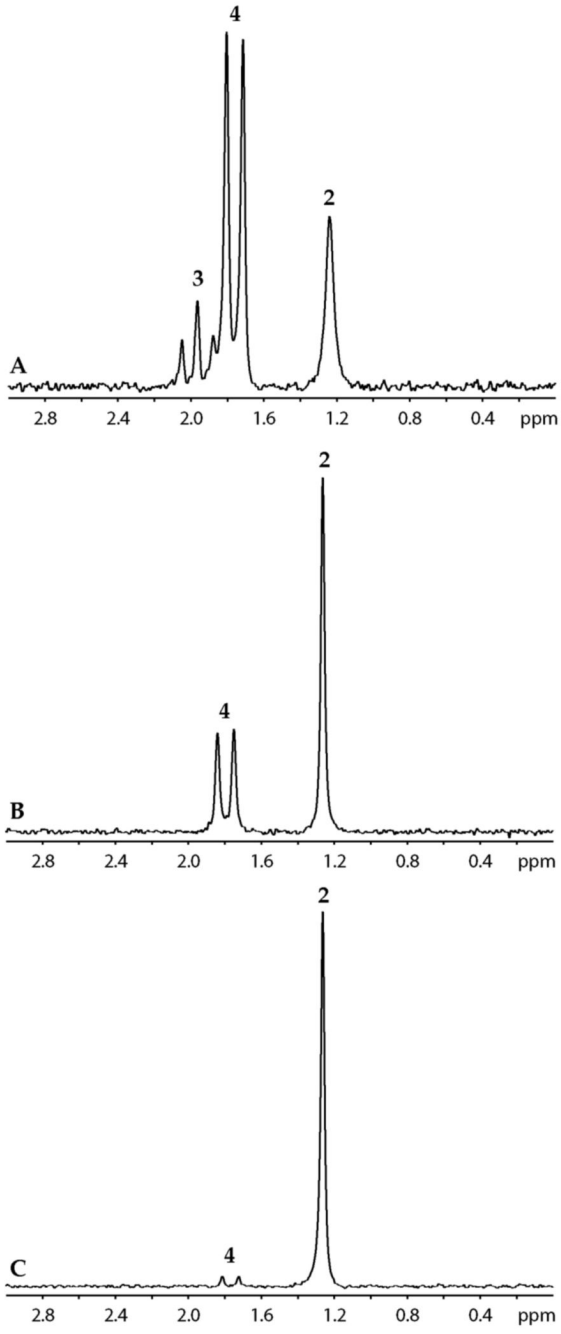

Figure 3.
^{6}Li NMR spectrum of 0.10 M [^{6}Li,^{15}N]LDA at −90 °C with (A) 0.050 M **1**; (B) 0.10 M **1**; (C) 0.10 M **1** at −90 °C after warming at −40 °C for 60 minutes.

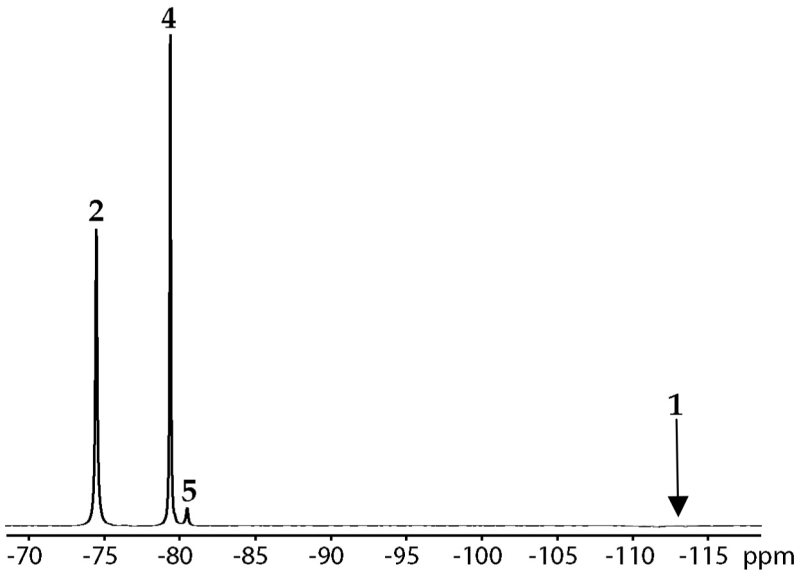

Figure 4.
^{19}F NMR spectrum of 0.10 M LDA with 0.10 M **1** at −78 °C.

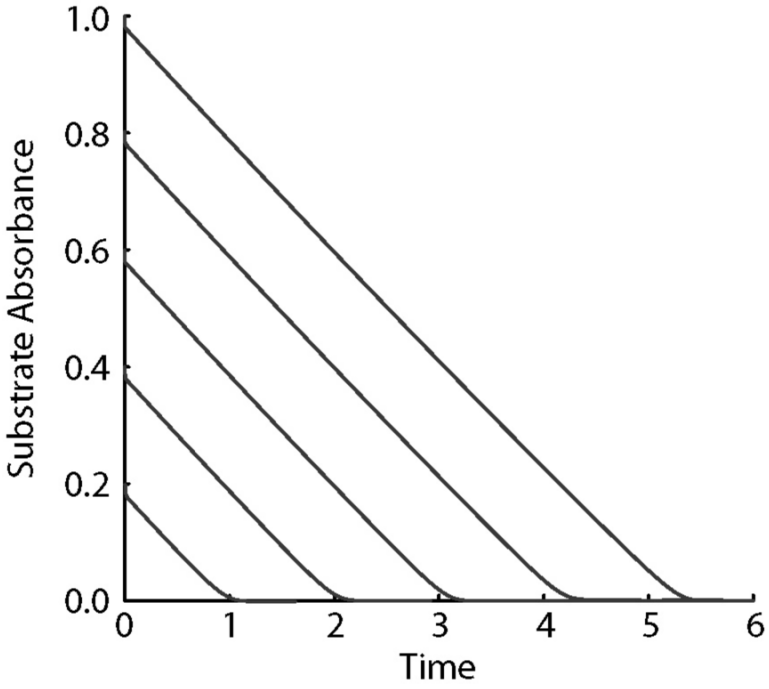

Figure 5.
Theoretical depiction of substrate dependence for a zeroth-order reaction.

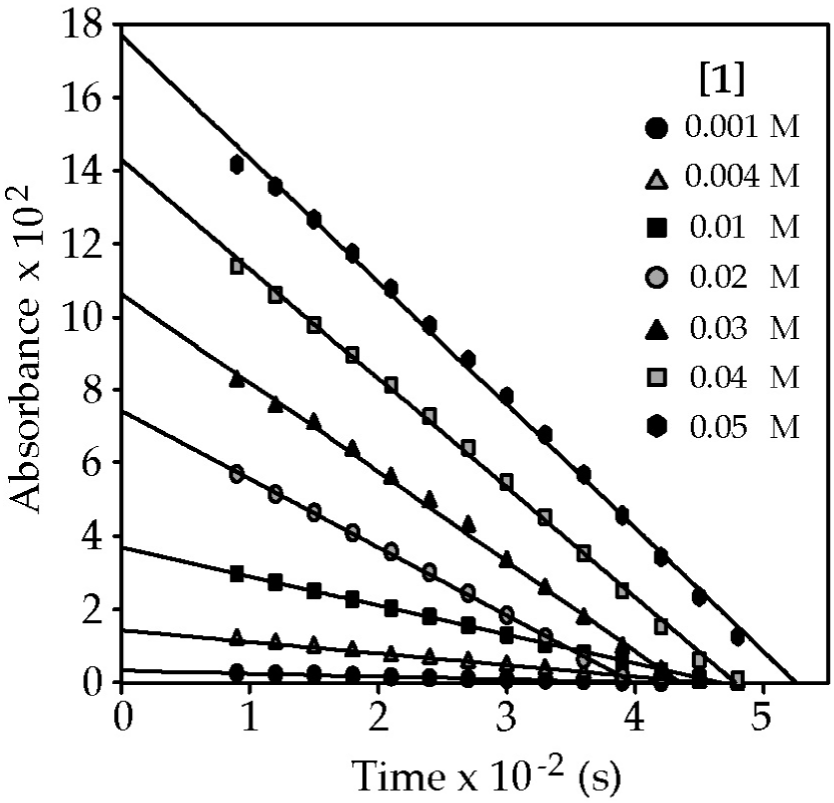

Figure 6.
Plot showing IR absorbance of **1** (1721 cm^{-1}) versus time for different initial concentrations of carbamate **1**.

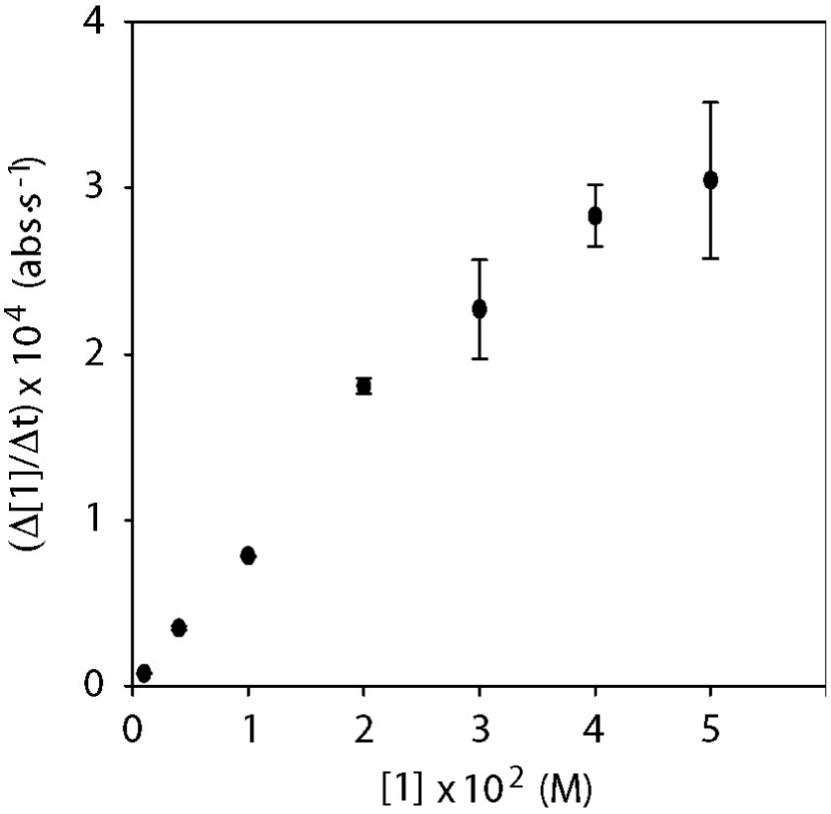

Figure 7.
Plot of Δ[**1**]/Δt (from Figure 6) versus [**1**] for the ortholithiation of **1** with 0.10 M LDA in 12.2 M THF/hexane cosolvent at −78 °C.

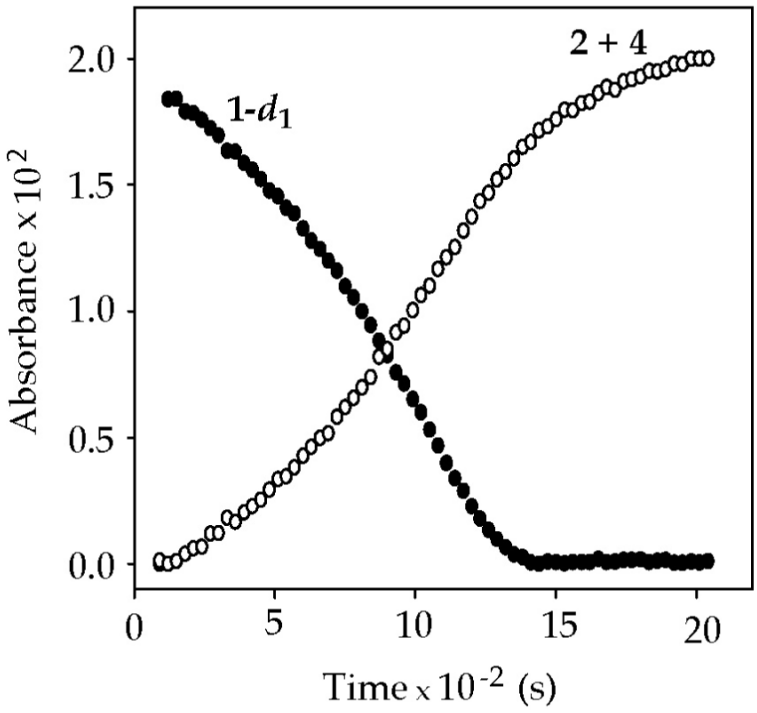

Figure 8.

Absorbance versus time for the reaction of (0.004 M) **1**−d_1 with (0.10 M) LDA in 12.2 M THF/hexane cosolvent at −78 °C. (**1**-d_1, 1721 cm^{-1}; **2 + 4**, 1660 cm^{-1})

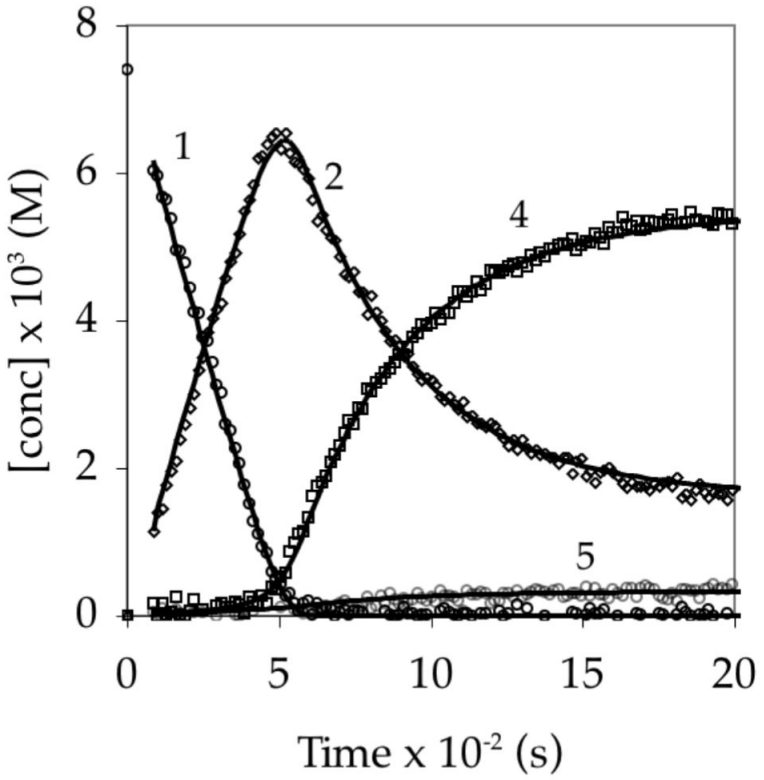

Figure 9.

Concentrations versus time for the reaction of 0.0074 M **1** with 0.10 M LDA in 12.2 M THF at −78 °C monitored by ^{19}F NMR spectroscopy. The functions result from a least squares fit to the model outline in eqs 9-12 and described mathematically by eqs 16-20.

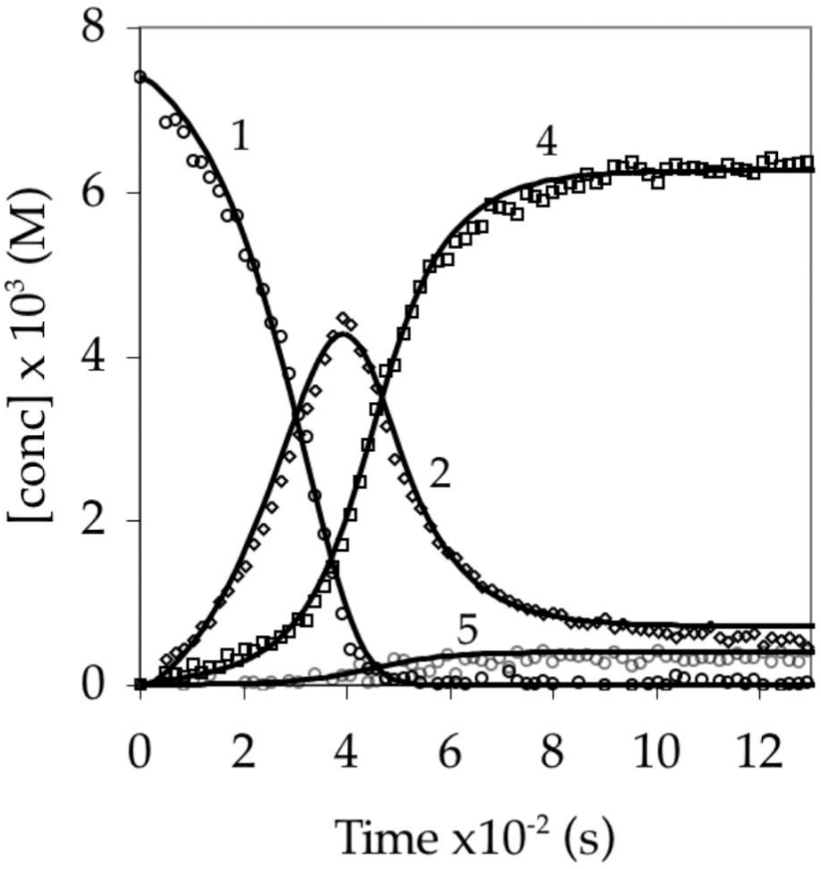

Figure 10.

Concentrations versus time for the reaction of 0.0074 M **1** with 0.10 M LDA in 4.9 M THF at −78 °C monitored by ^{19}F NMR spectroscopy. The functions result from a least squares fit to the model outline in eqs 9-12 and described mathematically by eqs 16-20.

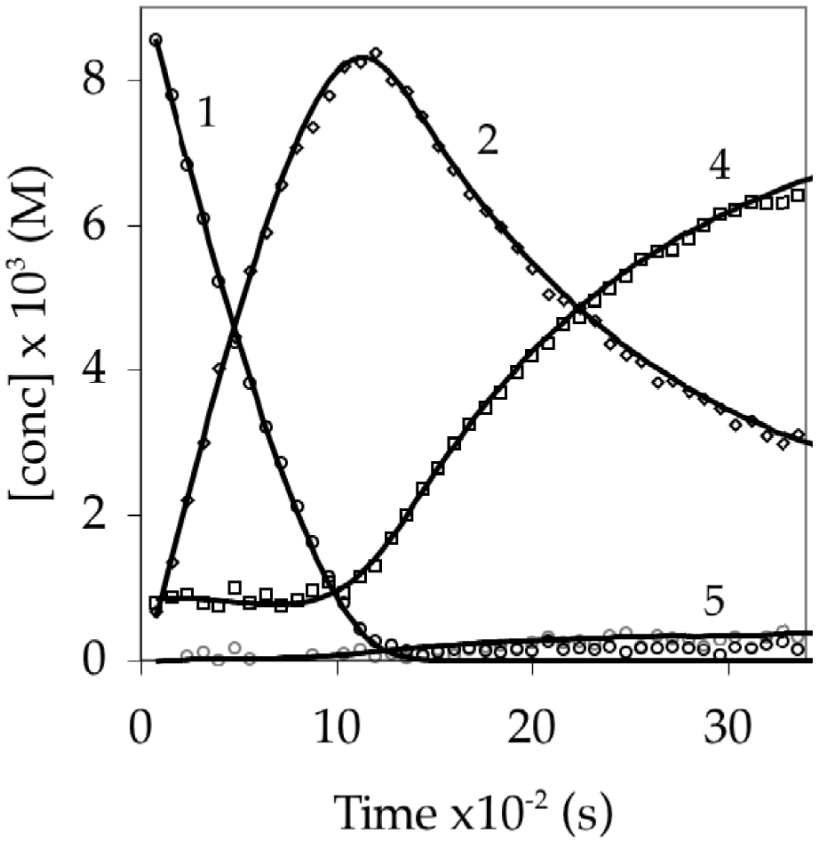

Figure 11.
Concentrations versus time for the reaction of 0.01 M **1** with 0.40 M LDA in 12.2 M THF at −100 °C monitored by ^{19}F NMR spectroscopy. The functions result from a least squares fit to the model outline in eqs 9-12 and described mathematically by eqs 16-20.

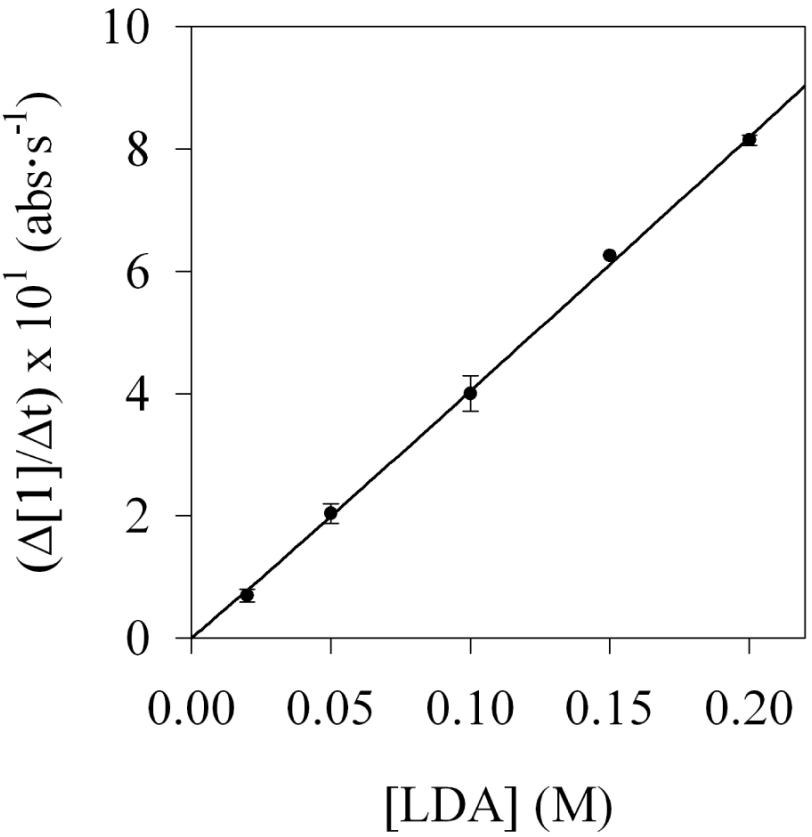

Figure 12.
Plot of initial rates versus [LDA] for the lithiation of carbamate **1** (0.0074 M) in 12.2 M THF at −78 °C. The curve depicts the result of an unweighted least-squares fit to *rate* = k[LDA]^n (k = (4.2 ± 0.2) × 10^1; n = 1.02 ± 0.03).

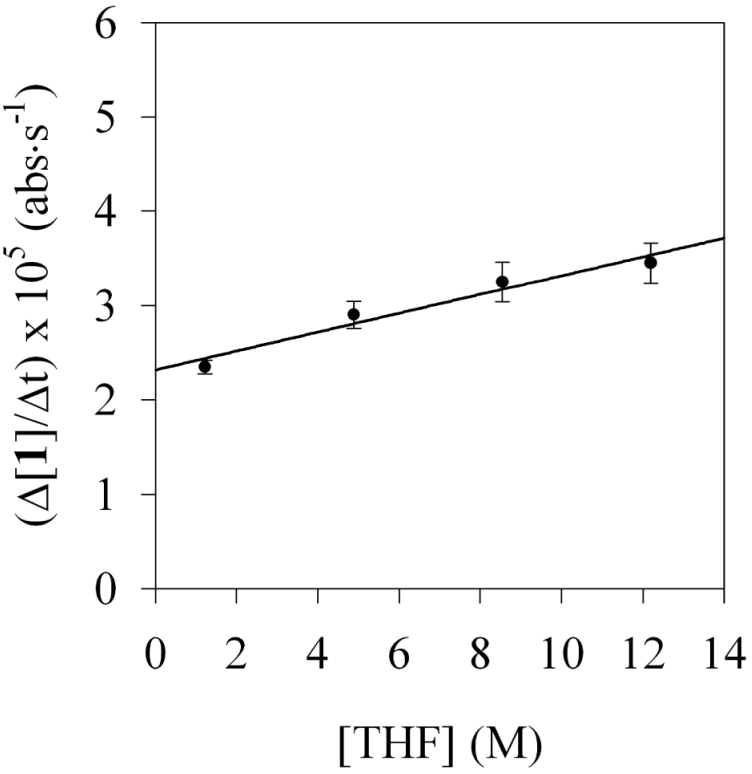

Figure 13.
Plot of initial rates versus [THF] for the lithiation of carbamate **1** (0.004 M) in 0.1 M LDA using hexanes as cosolvent at −78 °C. The curve depicts the result of an unweighted least-squares fit to *rate* = k[THF] + k' (k = (1.0 ± 0.2) × 10^{-6}; k' = 2.3 ± 0.1) × 10^{-5}).

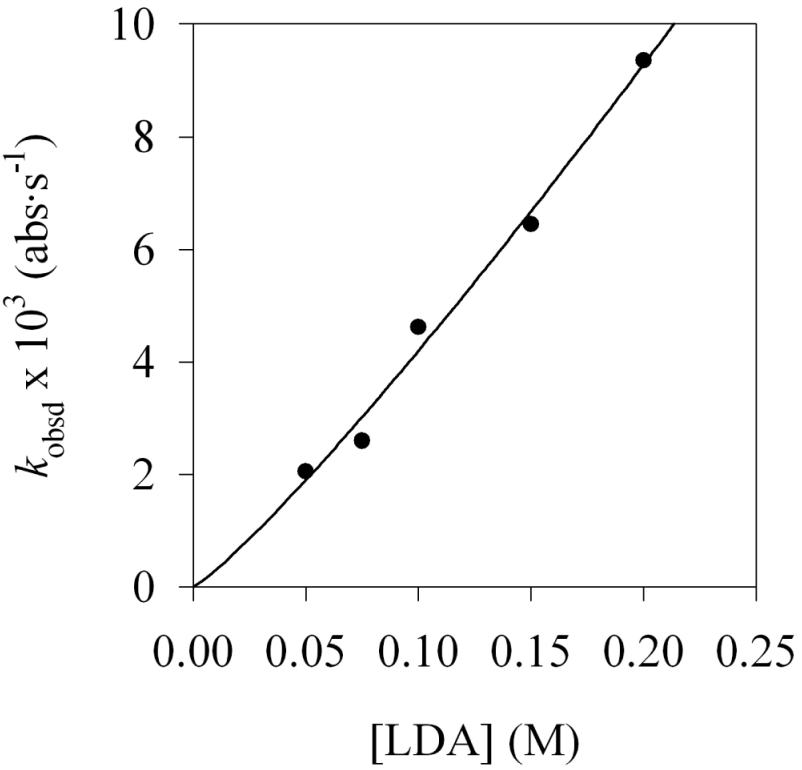

Figure 14.
Plot of k_{obsd} versus [LDA] for the condensation of LDA with aryllithium **2** (0.0074 M) in 12.2 M THF at −78 °C. The curve depicts the result of an unweighted least-squares fit to $k_{obsd} = k[LDA]^n + c$ ($k = (60 \pm 10)$; $n = 1.1 \pm 0.1$).

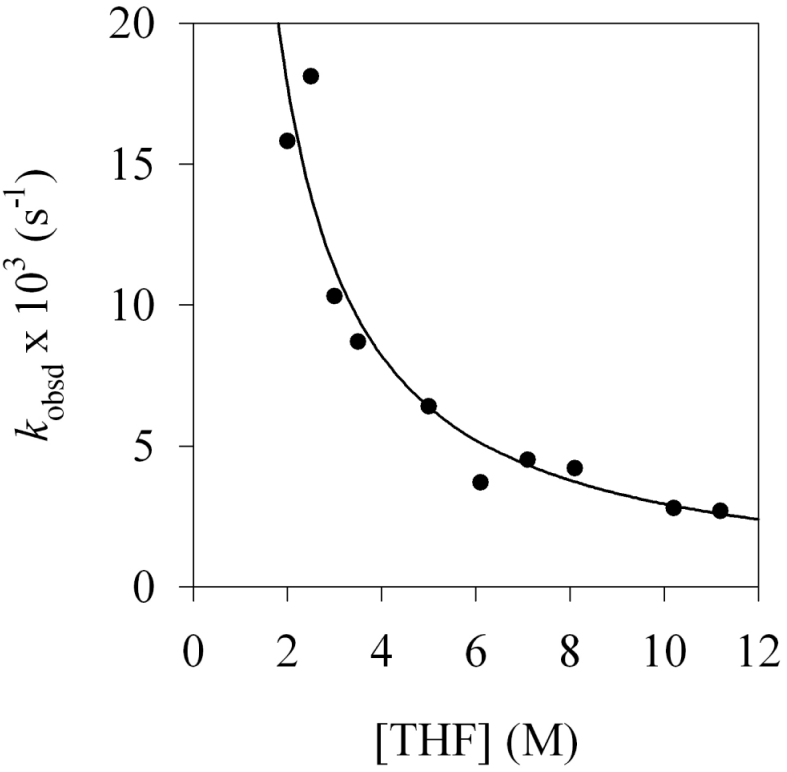

Figure 15.

Plot of k_{obsd} versus [THF] for the condensation of LDA with aryllithium **2** (0.0074 M) and 0.1 M LDA at −78 °C. The curve depicts the result of an unweighted least-squares fit to $k_{obsd} = k[THF]^n$ ($k = (39 \pm 7)$; $n = -1.1 \pm 0.2$).

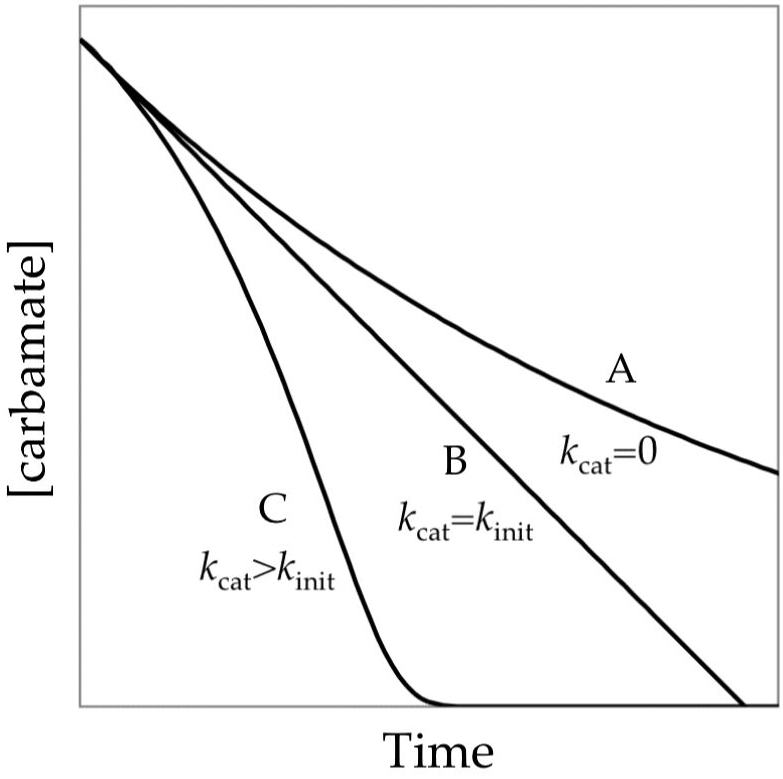

Figure 16.
Influence of autocatalysis on the LDA-mediated metalation of carbamate **1** as described in eqs 9-12.